

# Electron-Transporting Semi-Rigid Polyester-Imides Made up of a Tetracarboxdiimide of *p*-Terphenyl Analogue of 1,3,4-Oxadiazole: Preparation, and Thermal, Optical, and Electrochemical Properties

Moriyuki Sato, Mutsumi Inata, Isao Yamaguchi

Department of Materials Science, Faculty of Science and Engineering, Shimane University, Matsue, Shimane 690-8504, Japan

Received 24 November 2011; accepted 31 January 2012

DOI 10.1002/app.36956

Published online in Wiley Online Library (wileyonlinelibrary.com).

**ABSTRACT:** Electron-transporting semi-rigid polyester-imides composed of a tetracarboxdiimide (2,5-di(3,4-dicarboxyphthalimido)-1,3,4-oxadiazole; DDPOD) of *p*-terphenyl analogue of 1,3,4-oxadiazole were successfully prepared by the melt polycondensation of a monomer, a dialcohol derivative of DDPOD, with four diesters in the presence of zinc acetate as a catalyst, and their thermal, UV-vis absorption, photoluminescent (PL) and electrochemical properties were examined. The structures of the resulting polymers were characterized by Fourier transform infrared and <sup>1</sup>H NMR spectroscopies and elemental analyses. Differential scanning calorimetry measurements, X-ray diffraction analyses and polarizing microscope observations suggested that the polymers prepared from aliphatic diesters formed highly ordered thermotropic liquid crystalline smectic phases. The UV-vis and PL spectra in the solutions and in the films displayed that the obtained polymers showed

absorption and bluish violet-light emissions based on the DDPOD moiety. Cyclic voltammetry measurements revealed that these polymers had more stable HOMO levels and were more sensitive to oxidation than polymers comprising electron-accepting 2,5-diphenyl-1,3,4-oxadiazole in the backbones. The DDPOD unit brought the extension of differences between electron-injection and hole-injection barriers in the polymers. It was found that the polymers containing the DDPOD unit in the main chains in this study not only showed bluish violet light-emitting properties but also behaved as electron-transporting materials for organic electroluminescent devices. © 2012 Wiley Periodicals, Inc. *J Appl Polym Sci* 000: 000–000, 2012

**Key words:** polymer synthesis and characterization; thermal properties; UV-vis spectroscopy; luminescence; electrochemistry

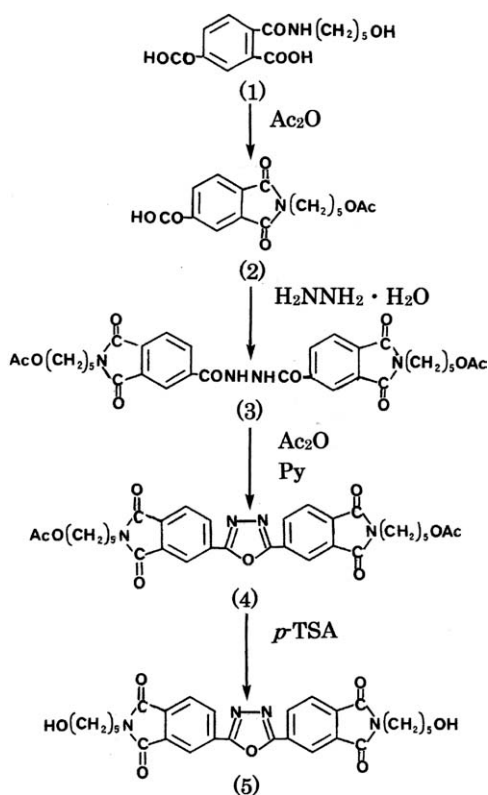
## INTRODUCTION

It is well known that polyimides have not only excellent mechanical, thermal, and chemical stabilities, but also various interesting physical properties such as photoluminescent (PL), electroluminescent (EL), nonlinear optical and liquid crystalline (LC) properties,<sup>1–15</sup> which are built up of electron-donating and -withdrawing well-defined conjugation units.<sup>4–6</sup> They have the potential to be light-emitting and electron-transporting materials for EL devices. We found that semi-rigid polyester-imides having 3,3',4,4' -*p*-terphenyltetracarboxdiimide ring show a blue-light emission in solutions and in films in addition to thermotropic LC properties.<sup>7</sup> Semi-rigid polyester-imides composed of 3,3',4,4'-biphenyltetracarboxdiimide with benzene ring next to the imide unit formed enantiotropic smectic phases.<sup>8</sup> A polypyro-

mellitimide composed of quaterphenyl analogue of 2,2'-bifuryl with a blue-light emission in a high quantum yield was developed.<sup>9</sup> Polyimides containing *N*-phenyl-1,8-naphthalimide ring, which acts as laser media, in the main chain were found to display EL properties with green and yellow emissions in the film.<sup>10</sup> Poly(perylene bismaleimide)s composed of biphenyl and anthracene groups had excellent thermal and chemical stabilities, and relatively high quantum yields with a red-light emission.<sup>12</sup> *N*-substituted maleimide-conjugated polymers showed good thermal and PL properties with yellow-to-light blue emissions.<sup>15</sup>

On the other hand, aromatic 1,3,4-oxadiazole (ODA) derivatives are used as electron-transporting and light-emitting materials for EL devices.<sup>16–19</sup> Some ODA derivatives showed thermotropic LC phases although the potential of LC properties was low.<sup>20</sup> Their aromatic derivatives formed stable thermotropic LC phases despite a bent molecular structure.<sup>21</sup> Multifunctional thermotropic LC compounds composed of a quaterphenyl analogue of ODA were reported to show high electron mobility and

Correspondence to: M. Sato (msato@riko.shimane-u.ac.jp).



Scheme 1 Synthesis of monomer 5.

polarized EL properties.<sup>22</sup> In recent years, it was disclosed that 2,5-diphenyl-1,3,4-oxadiazole (DPOD) acts as a relative electron donor compared with maleimide or itaconimide,<sup>23,24</sup> having a stronger electron-accepting ability,<sup>25</sup> although the DPOD is generally recognized as an electron-accepting compound.<sup>13,16</sup> In polyimides made up of DPOD and phthalimide (PI) rings, the former behaves as an electron donor and the latter as an electron acceptor.<sup>13,25</sup> Therefore, it is expected that polymers composed of imide derivatives of DPOD have a conjugation unit and show an electron-transporting property arising from the DPOD and PI rings in addition to LC and PL properties.

In this article, new semi-rigid polyester-imides 7 composed of a tetracarboxydiimide of *p*-terphenyl analogue of ODA, 2,5-di(3,4-dicarboxyphthalimido)-1,3,4-oxadiazole (DDPOD) moiety, were prepared from 2,5-bis[3,4-{*N*-(5-hydroxypentamethylene)dicarboxyphthalimido}]1,3,4-oxadiazole 5 and four diesters 6 by melt polycondensation in the presence of zinc acetate as a catalyst (Scheme 1) and their thermal, optical, and electrochemical properties were evaluated. Polyester-imides 7 with a DDPOD unit will show visible light-emitting and electron-transporting properties together with LC properties, because both the DPOD and the PI units (DDPOD moiety) coexist in the polymer backbones. The monomer 5, a dihydroxy derivative of DDPOD,

was synthesized using *N*-(5-acetoxypentamethylene) derivative 2 of trimellitimide via imidation and acylation of an intermediate amido-carboxylic acid 1 prepared from trimellitic anhydride (TA) and 5-amino-1-pentanol (AP) as starting materials (Scheme 2).

## EXPERIMENTAL

### Materials

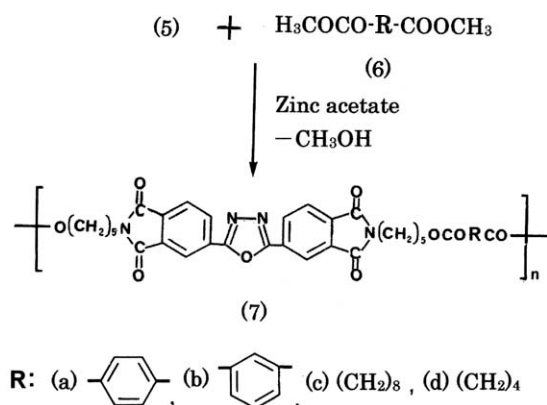
TA, AP, lithium chloride, hydrazine monohydrate, *p*-toluenesulfonic acid (*p*-TSA), *tetra-n*-butylammonium perchlorate (TBAP), silver nitrate, and zinc acetate were commercially available and used as received. *N,N*-dimethylacetamide (DMAc), *N*-methyl-2-pyrrolidone (NMP), pyridine, acetic anhydride, and triphenyl phosphite (TPP) were purified by vacuum distillation. Chloroform, 1,4-dioxane, ethanol, and methanol were used after purification via distillation. Dimethyl terephthalate 6a, dimethyl isophthalate 6b, dimethyl sebacate 6c, and dimethyl adipate 6d were purified by recrystallization.

### Monomer synthesis

#### 3,4-[*N*-(5-Acetoxypentamethylene)] carboxytrimellitimide 2

AP (0.05 mol, 5.16 g) was added to a DMAc solution (30 mL) of TA (0.05 mol, 9.61 g) and stirred for 1 h in ice-water to yield intermediate 1. To the solution, acetic anhydride (16 mL) and pyridine (4 mL) were added and the solution was refluxed for 5 h. After the reaction, the resulting solution was poured into an excess of water to precipitate the desired compound. The precipitate was filtered off, washed thoroughly with water three times, and recrystallized from a mixture of water and methanol (*v/v* = 1/1) three times. Dried at 60°C *in vacuo* for a day gave the imide compound 2 in a yield of 66%.  $M_p = 120\text{--}122^\circ\text{C}$ .

Fourier transform infrared (FTIR) (KBr,  $\text{cm}^{-1}$ ): 2860–2960 (CH stretching), 1780, 1710 (imide C=O),



Scheme 2 Synthesis of polymers 7.

1725 (AcO), 1700 (C(O)OH, shoulder), 725 (imide ring).

ELEM. ANAL., Calcd. for  $C_{16}H_{17}NO_6$  (319.2): C, 60.21%; H, 5.33%; N, 4.39%. Found: C, 59.94%; H, 5.33%; N, 3.93%.

#### 2,5-Bis[3,4-[N-(5-acetoxypentamethylene)dicarboxphthalimido]]-1,3,4-oxadiazole 4

To a solution of lithium chloride (0.07 mol, 2.97 g) dissolved in NMP (165 mL) hydrazine monohydrate (16.5 mmol, 0.83 g), TPP (33 mmol, 10.24 g) and compound 2 (33 mmol, 10.54 g) were added. The mixture was heated at 120°C for 5 h under a nitrogen atmosphere. The reaction solution was poured into an excess of water to precipitate the solid. The precipitate 3 was washed with water three times and dried at 60°C in a vacuum. Yield: 77%.  $M_p = 212^\circ\text{C}$ . The intermediate compound 3 (3.15 mmol, 2.00 g) was heated in a mixture of acetic anhydride (6 mL) and pyridine (2 mL) under reflux for 7 h. The reaction solution was evaporated to dryness. The resulting solid was recrystallized from ethanol three times and dried at 60°C *in vacuo* overnight. Yield: 27%.  $M_p = 149\text{--}150^\circ\text{C}$ .

FTIR (KBr,  $\text{cm}^{-1}$ ): 2840–2970 (CH stretching), 1770, 1710 (imide C=O), 1730 (AcO), 1560 (C=N), 725 (imide ring).

ELEM. ANAL., Calcd. for  $C_{32}H_{32}N_4O_9$  (616.4): C, 62.35%; H, 5.19%; N, 9.09%. Found: C, 62.37%; H, 5.24%; N, 8.94%.

#### 2,5-Bis[3,4-[N-(5-hydroxypentamethylene)dicarboxphthalimido]]-1,3,4-oxadiazole 5

The compound 4 (8.00 mmol, 0.52 g) was refluxed in a mixture of 1,4-dioxane (3 mL) and methanol (1 mL) for 5 h in the presence of *p*-TSA (0.04 g) as a catalyst. After the reaction, the solution was cooled and the separated crystal was filtered off. Recrystallization from a mixture of 1,4-dioxane and methanol (v/v = 2/8) three times, and being dried at 60°C in a vacuum for 1 day, afforded the oxadiazole compound 5 in a yield of 24%.  $M_p = 194\text{--}195^\circ\text{C}$ .

FTIR (KBr,  $\text{cm}^{-1}$ ): 3320 (OH stretching), 2840–2960 (CH stretching), 1770, 1710 (imide C=O), 1560 (C=N), 725 (imide ring).  $^1\text{H}$  NMR ( $\text{CDCl}_3$ ,  $\delta$ , ppm): 8.59–8.60 (d, 4H, aromatic protons), 8.05 (d, 2H, aromatic protons), 3.75 (m, 4H,  $\text{NCH}_2$ ), 3.65 (m, 4H,  $\text{CH}_2\text{OH}$ ), 1.4–1.8 (m, 12H, aliphatic chains).

ELEM. ANAL., Calcd. for  $C_{28}H_{28}N_4O_7$  (532.5): C, 63.17%; H, 5.26%; N, 10.53%. Found: C, 63.00%; H, 5.36%; N, 9.94%.

#### Preparation of polyester-imides 7

A typical example for the preparation of polymer 7c is described. Monomer 5 (0.451 mmol, 0.24 g) and

dimethyl sebacate (6c) (0.675 mmol, 0.155 g) were heated at 200°C for 5 h in the presence of zinc acetate (5 mg) as a catalyst in nitrogen. The reaction mixture was heated at 200°C for 30 min at a pressure of 20 Torr, and then stirred for further 30 min at a pressure below 3 Torr. After the resulting solid was dissolved in chloroform, the chloroform solution was poured into methanol to precipitate the polymer 7c. The precipitate was filtered off, washed with water, refluxed in methanol three times, and dried at 60°C *in vacuo* overnight. Yield: 68%.

FTIR (KBr,  $\text{cm}^{-1}$ ): 2850–2940 (CH stretching), 1770, 1710 (imide C=O), 1735 (shoulder, ester C=O), 1560 (C=N), 725 (imide ring).  $^1\text{H}$  NMR ( $\text{CDCl}_3$ ,  $\delta$ , ppm): 8.59–8.61 (d, 4H, aromatic protons), 8.05 (d, 2H, aromatic protons), 4.3–4.4 (d, 4H,  $\text{CH}_2\text{OC}(\text{O})$ ), 3.7–3.8 (m, 4H,  $\text{NCH}_2$ , and  $\text{CH}_2\text{OH}$ ), 2.28 (d, 4H,  $\text{OC}(\text{O})\text{CH}_2$ ), 1.2–1.9 (m, 24H, aliphatic chains). Characterization data for the other polymers 7a, 7b, and 7d were shown.

7a: FTIR (KBr,  $\text{cm}^{-1}$ ): 2860–2940 (CH stretching), 1770, 1715 (overlapped imide and ester C=O), 1550 (C=N), 725 (imide ring).  $^1\text{H}$  NMR ( $\text{CDCl}_3$ ,  $\delta$ , ppm): 8.60 (t, 4H, aromatic protons), 8.05 (d, 2H, aromatic protons), 4.25–4.4 (t, 4H,  $\text{CH}_2\text{OC}(\text{O})$ ), 3.72–3.82 (m, 4H,  $\text{NCH}_2$ ), 3.6–3.72 (m, 4H,  $\text{CH}_2\text{OH}$ ), 1.25–1.95 (m, 12H, aliphatic chains).

7b: FTIR (KBr,  $\text{cm}^{-1}$ ): 2850–2950 (CH stretching), 1770, 1715 (overlapped imide and ester C=O), 1550 (C=N), 730 (imide ring).  $^1\text{H}$  NMR ( $\text{CDCl}_3$ ,  $\delta$ , ppm): 8.56 (m, 6H, aromatic protons), 8.21 (d, 2H, aromatic protons), 8.04 (t, 2H, aromatic protons), 4.25–4.4 (t, 4H,  $\text{CH}_2\text{OC}(\text{O})$ ), 3.73–3.84 (m, 4H,  $\text{NCH}_2$ ), 3.55–3.73 (m, 4H,  $\text{CH}_2\text{OH}$ ), 1.2–1.95 (m, 12H, aliphatic chains).

7d: FTIR (KBr,  $\text{cm}^{-1}$ ): 2860–2940 (CH stretching), 1770, 1710 (overlapped imide and ester C=O), 1555 (C=N), 725 (imide ring).  $^1\text{H}$  NMR ( $\text{CDCl}_3$ ,  $\delta$ , ppm): 8.60 (t, 4H, aromatic protons), 8.05 (d, 2H, aromatic protons), 3.9–4.14 (t, 4H,  $\text{CH}_2\text{OC}(\text{O})$ ), 3.55–3.85 (m, 4H,  $\text{NCH}_2$ , and  $\text{CH}_2\text{OH}$ ), 2.32 (s, 4H,  $\text{OC}(\text{O})\text{CH}_2$ ), 1.2–1.95 (m, 16H, aliphatic chains).

#### Measurements

$^1\text{H}$  NMR spectra were recorded with a JEOL LMN EX270 spectrometer in  $\text{CDCl}_3$ . FTIR spectra were obtained on a Jasco FT/IR 5300 spectrometer by the KBr disk method. Differential scanning calorimetry (DSC) measurements were carried out with a Shimadzu DSC-60 calorimeter at a heating and a cooling rate of  $10^\circ\text{C min}^{-1}$  in nitrogen. X-ray analyses of the polymers quenched from the LC states were undertaken with a Rigaku Denki RINT 2200 generator with  $\text{CuK}\alpha$  irradiation. Polarizing microscope observations were performed with a polarized microscope (Nikon) equipped with a hot plate (magnification: 200 $\times$ ). The UV–vis absorption and PL



TABLE I  
Synthetic Results of Polyester-Imides 7

Polym. no.	Yield (%)	$M_n^a$	$M_w/M_n^a$	$T_g^b$	Elemental formula (formula weight)	Elemental analysis (%)			
						C	H	N	
7a	54	4300	1.30	89	$(C_{36}H_{30}O_9N_4)_n$ (662.40) <sub>n</sub>	Calcd.	65.27	4.53	8.46
						Found	63.12	4.85	8.90
7b	41	4400	1.24	98	$(C_{36}H_{30}O_9N_4)_n$ (662.40) <sub>n</sub>	Calcd.	65.27	4.53	8.46
						Found	63.30	4.95	9.04
7c	88	9200	2.20	–	$(C_{38}H_{42}O_9N_4)_n$ (698.42) <sub>n</sub>	Calcd.	65.34	6.01	8.02
						Found	63.77	5.73	7.10
7d	51	5300	1.84	84	$(C_{34}H_{34}O_9N_4)_n$ (642.38) <sub>n</sub>	Calcd.	63.57	5.29	8.72
						Found	61.15	5.11	8.12

<sup>a</sup>  $M_n$ : number-average molecular weight;  $M_w/M_n$ : molecular weight distribution.

<sup>b</sup> Glass transition temperature.

spectra were measured in chloroform solutions and in the films on a Jasco UVIDE C-510 spectrophotometer and on a Hitachi 850 fluorescence spectrophotometer, respectively. Cyclic voltammetry (CV) measurements of polymers 7 were performed using an electrochemical analyzer (BAS 100 B/W) in acetonitrile with 0.1 mol L<sup>-1</sup> TBAP as the supporting electrolyte at a sweeping rate of 100 mV s<sup>-1</sup>. Potentials were measured against an Ag/Ag<sup>+</sup> (0.01 mol L<sup>-1</sup> AgNO<sub>3</sub>) reference electrode with ferrocene as the internal standard. The onset potentials were estimated from the intersection of two tangents drawn at the rising current and background current of the CV. The number-average molecular weight ( $M_n$ ) and  $M_w/M_n$  values were estimated by size exclusion chromatography with a Jasco 830-RI refractometer and a column combination (K-803/K-804) (Shodex) with polystyrene standards in chloroform as an eluent.

## RESULTS AND DISCUSSION

### Preparation of monomer 5 and polyester-imides 7

Imidation and acylation of an intermediate amidocarboxylic acid 1, which was derived from TA and AP, in acetic anhydride gave a *N*-(5-acetoxypentamethylene) derivative 2 of trimellitimide. Phosphorylation of the monoacetoxy derivative 2 with hydrazine monohydrate using TPP and lithium chloride in NMP afforded a corresponding hydrazide derivative 3 of trimellitimide, followed by preparation of a bisacetoxy compound 4 of DDPOD by cyclodehydration of the compound 3 in acetic anhydride including pyridine. A monomer 5, a diol derivative of DDPOD for melt polycondensation, was synthesized by hydrolysis of the bisacetoxy derivative 4 of DDPOD in the presence of *p*-TSA. FTIR spectra of compounds 2–5 showed absorption bands based on the imide ring at 725, 1710, and 1770 cm<sup>-1</sup> together with CH stretching bands at 2840–2970 cm<sup>-1</sup>. In the FTIR

spectrum of compound 5, the absorption of acetoxy carbonyl for compound 4 at 1720 cm<sup>-1</sup> vanished, and the OH stretching band appeared at around 3300 cm<sup>-1</sup>. Compounds 4 and 5 also displayed an absorption band owing to C=N of the ODA ring at 1560 cm<sup>-1</sup>. The <sup>1</sup>H NMR spectrum of monomer 5 in CDCl<sub>3</sub> showed proton signals of the aromatic ring at 8.0–8.6 ppm, NCH<sub>2</sub> signals neighboring the imide ring at 3.7–3.8 ppm, CH<sub>2</sub>OH groups at 3.6–3.7 ppm, and (CH<sub>2</sub>)<sub>4</sub> chains at 1.4–1.8 ppm. The elemental analysis data for compounds 2, 4, and 5 were in agreement with the calculated values. These data support the formation of compounds 2–5.

Polyester-imides 7 having both DPOD and PI units (DDPOD moiety) in the backbones were successfully prepared from monomer 5 and diesters 6 using zinc acetate as a catalyst by melt polycondensation, whose  $M_n$  and  $M_w/M_n$  values were 4300–9200 and 1.21–2.20, respectively. The polyester-imides 7 were readily soluble in chloroform and films were able to be cast from the chloroform solutions although their molecular weights were not very high. Synthetic results for the polyester-imides 7 are summarized in Table I. The FTIR spectra of polymers 7 showed characteristic absorption bands based on imide C=O at 1710 and 1770 cm<sup>-1</sup>, C=N of the ODA ring at 1560 cm<sup>-1</sup> and the imide ring at 725 cm<sup>-1</sup>, but the absorptions of ester C=O were observed with difficulty because of overlapping with those of imide C=O. In the <sup>1</sup>H NMR spectra of polymers 7a and 7b in CDCl<sub>3</sub>, CH<sub>2</sub>OC(O) proton signals at 4.3–4.4 ppm were observed as well as signals detected in the monomer 5. The <sup>1</sup>H NMR spectra of polymers 7c and 7d displayed signals owing to OC(O)CH<sub>2</sub> protons at 2.28 ppm in addition to the above-described signals. Typical <sup>1</sup>H NMR spectrum for polymer 7a in CDCl<sub>3</sub> is shown in Figure 1. Elemental analysis values agree with the calculated ones as listed in Table I, although the carbon values are slightly low compared with the calculated ones because of the presence of unreacted terminal

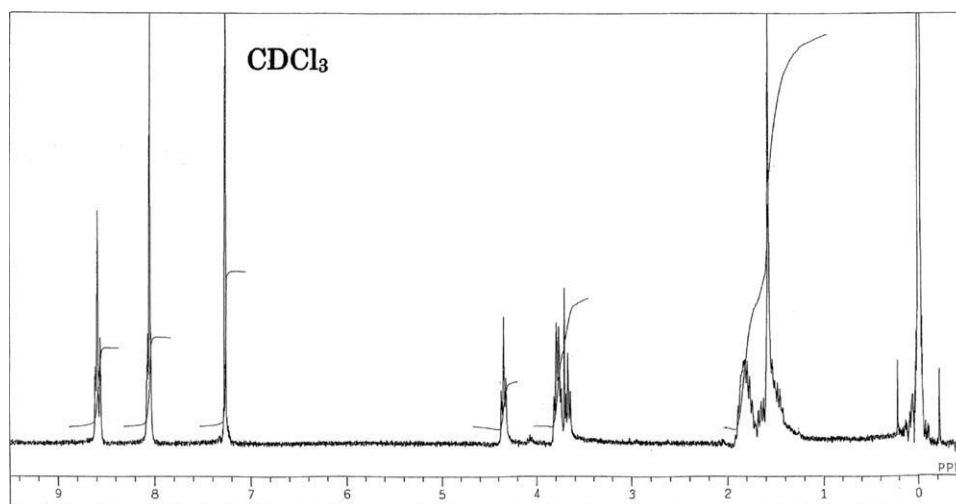


Figure 1 Typical  $^1\text{H}$  NMR spectrum for polymer 7a in  $\text{CDCl}_3$ .

groups in the polymer backbones. These spectral data and elemental analysis values support the production of expected polyester-imides 7 having DDPOD moiety in the backbones.

#### Thermal properties of polyester-imides 7

The thermal properties of polyester-imides 7 were evaluated by DSC measurements, polarizing microscope observations, and X-ray diffraction (XRD) analyses. The polymers 7 were expected to show thermotropic LC phases, as they had a tetracarbox-diimide (DDPOD unit) of *p*-terphenyl analogues of

ODA in the backbone. In Figure 2, the DSC curves of polyester-imides 7 during the second heating runs are shown. The polymers 7c and 7d from the aliphatic diesters 6c and 6d show two endothermic peaks based on the solid-to-LC phase ( $T_m$ ) and LC phase-to-isotropization ( $T_i$ ) in addition to glass transition temperatures ( $T_g$ ) near 90°C. The polymer 7d also displays an exotherm owing to crystallization at 123°C. The powder XRD patterns suggested that the polymers 7c and 7d form thermotropic LC phases between  $T_m$  (156°C for 7c and 146°C for 7d) and  $T_i$  (173°C for 7c and 160°C for 7d), although the typical texture (fine) was observed by polarizing microscope observations with difficulty. The powder XRD patterns of the polymers 7c and 7d, portrayed in Figure 3, show sharp reflections in the small ( $2\theta = 2.9\text{--}3.1^\circ$ ) and wide angles ( $2\theta = 16\text{--}30^\circ$ ), suggesting the formation of highly ordered smectic phases. 3D models of polymer 7b are shown in Figure 4 which indicate that the DDPOD unit has a linear and flat plate-like structure, that being a necessary condition for LC formation. In the DSC curves of polymers 7a and 7b

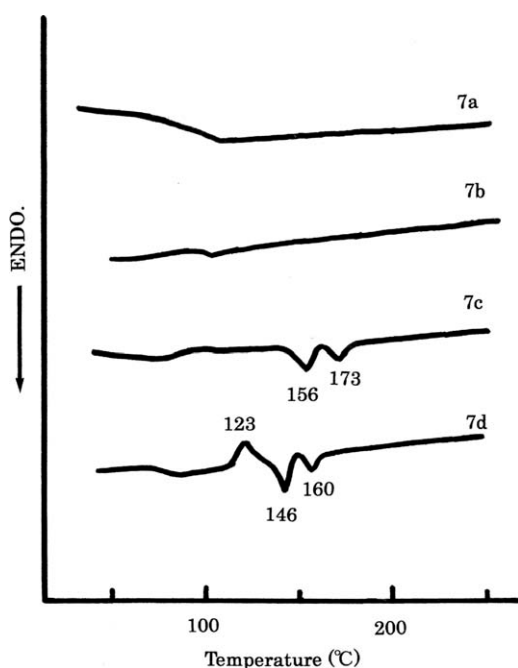


Figure 2 DSC curves of polyester-imides 7 on the second heating scans in nitrogen.

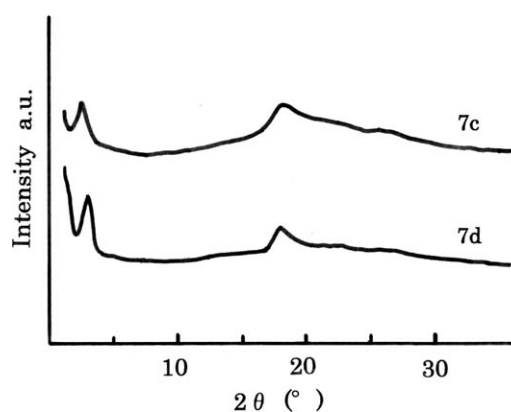
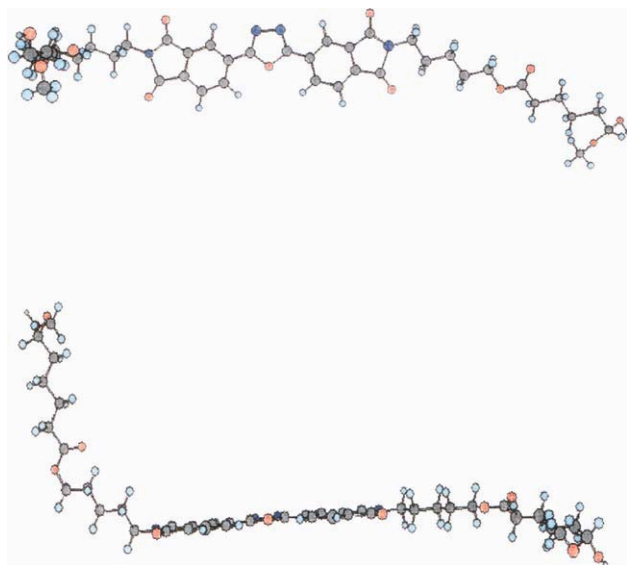


Figure 3 Powder XRD patterns of polymers 7c and 7d.



**Figure 4** 3D models of polymer 7d. [Color figure can be viewed in the online issue, which is available at [wileyonlinelibrary.com](http://wileyonlinelibrary.com).]

on the second heating runs, no endothermal peaks based on  $T_m$  and  $T_i$  are shown and only  $T_g$  steps were detectable. The LC phases were not observed in the polymers 7a and 7b, probably owing to the hindrance of the LC orientation by benzene rings.

### Optical properties of polyester-imides 7

UV-vis absorption and PL spectra of polyester-imides 7 composed of the DDPOD unit were examined in chloroform and in film. Their spectral data are summarized in Table II. Figure 5 shows the UV-vis absorption and the PL spectra of polymers 7 in films. The UV-vis spectra of polymers 7 in the chloroform solutions were normalized to the absorption peak maxima at 331.5–332 nm based on the  $\pi$ - $\pi^*$  electron transition of the DDPOD moiety. As summarized in Table II, the band gap energies ( $E_g^{\text{OPT}}$ ) of the polymers 7 estimated from extrapolated UV-vis absorption edges are 3.41–3.42 eV. In the solution, PL spectra of the polymers 7 when excited at 332 nm, the peak maxima were observed at 386–

389 nm with a bluish-violet emission, the Stokes shifts being 54.5–57.0 nm, whose values were almost the same as our previously reported hyperbranched polymers<sup>26</sup> composed of a phenylbenzothiadole moiety and higher than those of linear polyimides comprising DPOD and PI units.<sup>19</sup> The quantum yields ( $\Phi_{\text{PL}}$ ) of the polymers 7 measured in chloroform using coumarin 311 as a standard were 13–21% and comparable to those of block copolymers composed of an electron-transporting 2,5-diphenyl-1,3,4-thiadiazole (DPTD) unit.<sup>27</sup> The UV-vis spectra of polymers 7 in films displayed similar broad absorption curves, having absorption maxima at 326.5–332.5 nm as those in solutions. Their  $E_g^{\text{OPT}}$  values were 3.31–3.34 eV and lower than those in the solutions and for the polyimides comprising the DPOD and PI units.<sup>19</sup> In the PL spectra in films, when excited at 326.5–332.5 nm, the polymers 7 depicted peak maxima at 399.5–403.5 nm with a bluish-violet emission, which were observed at longer wavelengths of 13.5–15.5 nm than those in the chloroform solutions. The PL spectra of polymers 7 in films exhibited Stokes shifts of 70.0–74.0 nm, and were shifted to lower energies in comparison with the solution data, perhaps owing to intermolecular aggregation effects,<sup>28</sup> and their band edges being extended beyond 500 nm. Of the polymers 7, the polymers 7a and 7b from aromatic diesters showed PL emission maxima at higher wavelengths (lower band gap energies) than polymers 7c and 7d from aliphatic diesters. This might be owing to stronger intermolecular aggregation between the polymer chains with disubstituted benzene rings.<sup>28</sup> From these data, it is suggested that all the polyester-imides 7 emit bluish-violet light both in the solutions and in the films and show UV-vis absorption and PL peak maxima at higher wavelengths than polyimides composed of a DPOD unit.

### Electrochemical properties of polyester-imides 7

The electrochemical behaviors of the polyester-imides 7 having the DDPOD unit were examined using CV measurements of polymer films coated on a Pt electrode. The measurements were carried out

**TABLE II**  
UV-Vis and PL Spectral Data of Polyester-Imides 7 in Chloroform Solutions and in Films

Polym. no.	In solution					In film			
	$\lambda_{\text{max, abs}}$ (nm)	$\lambda_{\text{max, PL}}$ (nm)	$E_g^{\text{OPT}}$ (eV) <sup>a</sup>	$\Phi_{\text{PL}}$ <sup>b</sup> (%)	Stokes shift (nm)	$\lambda_{\text{max, abs}}$ (nm)	$\lambda_{\text{max, PL}}$ (nm)	$E_g^{\text{OPT}}$ (eV) <sup>a</sup>	Stokes shift (nm)
7a	332.0	387.0	3.42	13	55.0	332.5	402.5	3.31	70.0
7b	332.0	389.0	3.41	21	57.0	332.0	403.5	3.34	71.5
7c	331.5	386.0	3.42	14	54.5	326.5	400.5	3.34	74.0
7d	331.5	386.0	3.42	21	54.5	326.5	399.5	3.34	73.0

<sup>a</sup> Band gap energy calculated from UV-vis spectra.

<sup>b</sup> Quantum yield measured in chloroform using coumarin 311 as a standard.

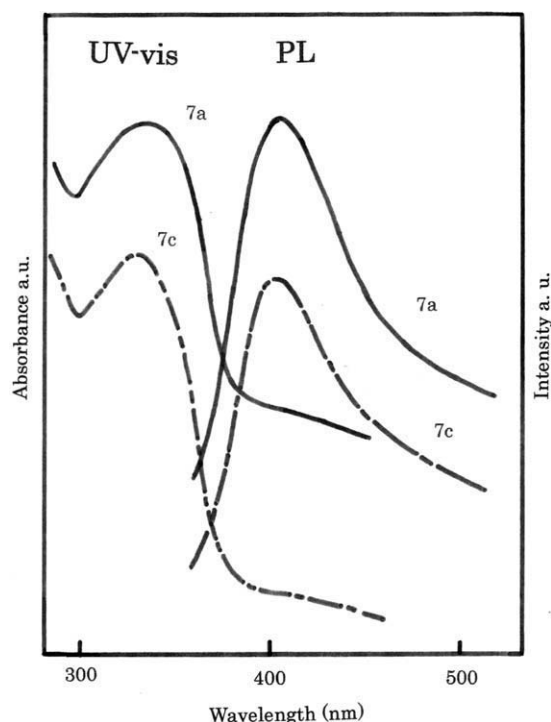


**Figure 5** UV-vis absorption and PL spectra of polyester-imides **7a** and **7c** in films.

in acetonitrile with TABP as a supporting electrolyte and with ferrocene as an internal standard. As shown in Figure 6, the polymer **7b** shows reversible reductions and irreversible oxidation. During an anodic sweep, onset oxidation potentials ( $E_{ox}$ :  $p$ -doping) were observed at 1.66 V, whereas onset reduction potentials ( $E_{red}$ :  $n$ -doping) were located near 1.54 V in the cathode sweep. The other polymers **7a**, **7c**, and **7d** showed CV behaviors analogous to the polymer **7b**. Aromatic polyimides derived from aromatic diamines and dianhydrides were reported to display different CV behaviors from these polymers **7**, where the reversible reduction process with the second or the third redox couple was recognized in the cathode sweep.<sup>29,30</sup> The  $E_{red}$  values of polymers **7** listed in Table III were almost the same as the first redox value of *N-n*-butylphthal-

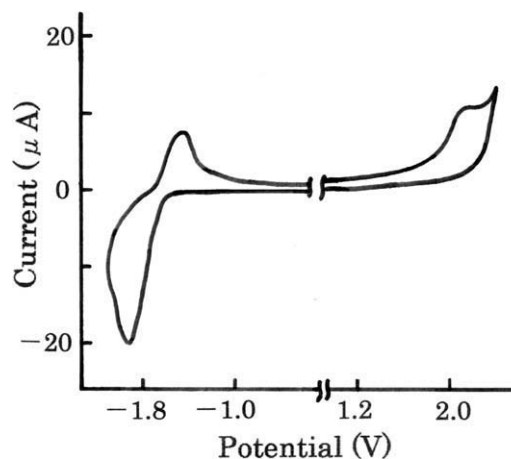


**Figure 6** CV curves of polyester-imide film **7b** in acetonitrile.

imide,<sup>30</sup> but the electrochemical behaviors of the polymers **7** appear to be different from those of the aromatic polyimides. We assumed that the reduction ( $n$ -doping) of the polymer films occurs more easily than the oxidation ( $n$ -dedoping), as the carriers injected in the polymers **7** having the DDPOD unit linked by aliphatic chains, composed of both the DPOD and the PI units, in the backbones are confined, and the mobility is lower for the oxidation than the reduction, perhaps owing to carrier adsorption and interactions with the polymers. Table III tabulates the reduction ( $E_{red}$ ) and oxidation ( $E_{ox}$ ) potential data, electrochemical band gap energy ( $E_g^{EC}$ ), optical band gap energy ( $E_g^{OPT}$ ) calculated from the absorption edges of UV-vis spectra, and LUMO and HOMO levels. On the basis of the  $E_{red}$ ,  $E_{ox}$ ,  $E_g^{OPT}$ , and  $E_g^{EC}$  values, we calculated the HOMO and LUMO energy values for the polymers **7** by assuming the energy level of the ferrocene reference (4.8 eV).<sup>31</sup> The oxidation process corresponds to the removal of charges from the HOMO level, whereas the reduction corresponds to the filling of the energy state by electrons to the LUMO level, that is, the ionization potential (IP) and electron affinity (EA), respectively. The HOMO and LUMO level values were estimated using the following formula:

**TABLE III**  
 $E_{red}$  and  $E_g$  Values, and HOMO and LUMO Energy Levels of Polyester-Imides **7** in Films

Polym. no.	$E_{red}$ vs. $E_{foc}$ (V) <sup>a</sup>	$E_{ox}$ vs. $E_{foc}$ (V) <sup>a</sup>	$E_g^{OPT}$ (eV) <sup>b</sup>	$E_g^{EC}$ (eV) <sup>c</sup>	LUMO (eV) <sup>d</sup>	HOMO (eV) <sup>e</sup>
<b>7a</b>	-1.53	1.65	3.31	3.18	-3.27	-6.58
<b>7b</b>	-1.56	1.64	3.34	3.20	-3.24	-6.59
<b>7c</b>	-1.44	1.65	3.34	3.09	-3.36	-6.70
<b>7d</b>	-1.42	1.66	3.34	3.08	-3.38	-6.72

<sup>a</sup>  $E_{foc} = 0.10$  V vs. Ag/Ag+.

<sup>b</sup> Determined from UV-vis spectra.

<sup>c</sup>  $E_g^{EC} = e(E_{ox} - E_{red})$ .

<sup>d</sup> LUMO (EA) =  $-e(E_{red} + 4.8)$ .

<sup>e</sup> HOMO (IP) = LUMO (EA) -  $E_g^{OPT}$ .



$$\text{LUMO (EA)} = -E_{\text{red}} - 4.8$$

$$\text{HOMO (IP)} = \text{LUMO (EA)} - E_g^{\text{OPT}}$$

The observed  $E_{\text{red}}$  values for polymers **7** were  $-1.42$  to  $-1.56$  V. The calculated values of HOMO (IP) levels of polymer films **7** were  $-6.58$  to  $-6.72$  eV and the LUMO (EA) level values were  $-3.24$  to  $-3.38$  eV. The  $E_g^{\text{OPT}}$  values were  $3.31$ – $3.34$  eV and almost the same as those given in our previous article,<sup>27,32</sup> which were in rough agreement with the electrochemical band gaps ( $E_g^{\text{EC}}$ :  $3.08$ – $3.20$  eV), differences in the  $E_{\text{ox}}$  and  $E_{\text{red}}$  values. The HOMO values of polymers **7** were lower than those of polymers composed of the DPTD unit,<sup>32</sup> DPOD-containing polyethers,<sup>33</sup> and PPV-based polymers.<sup>31</sup> The polyester-imides **7** were more sensitive to oxidation than the DPTD, DPOD, and PPV.<sup>31–33</sup> The LUMO level (EA) values of polymer **7** were lower than DPOD-containing polyethers ( $-2.76$  eV)<sup>33</sup> and *N*-phenylcarbazole-containing-PPV ( $-2.47$  eV),<sup>34</sup> but higher than those of poly(2-methoxy-1,4-phenylene vinylene) (PM-PPV) ( $-3.48$  eV).<sup>35</sup>

In Figure 7, energy band diagrams of polymers **7** for EL devices composed of ITO (anode) and Al (cathode) are shown. The energy difference between the LUMO levels of the polymers **7** and the work function of the cathode (Al:  $-4.3$  eV) corresponds to the electron-injection barrier ( $\Delta E_e$ ). Similarly, the hole-injection barrier ( $\Delta E_h$ ) is estimated as the energy difference between the HOMO levels of the polyester-imides **7** and the ITO anode ( $-4.8$  eV).<sup>36</sup> Table IV lists the barrier heights ( $\Delta E_e$  and  $\Delta E_h$ ) between the cathode (Al) or anode (ITO) and polyester-imides **7**. Tables III and IV and Figure 7 suggest that the energy barriers between the HOMO level values and ITO anode ( $-4.8$  eV) in the polymers **7** are larger than the DPTD-<sup>27</sup> and DPOD-containing polymers<sup>33</sup> and the differences in the barrier height ( $\Delta E_{\text{bh}} = \Delta E_e - \Delta E_h$ ) between  $\Delta E_e$  and  $\Delta E_h$  spread. The barriers of

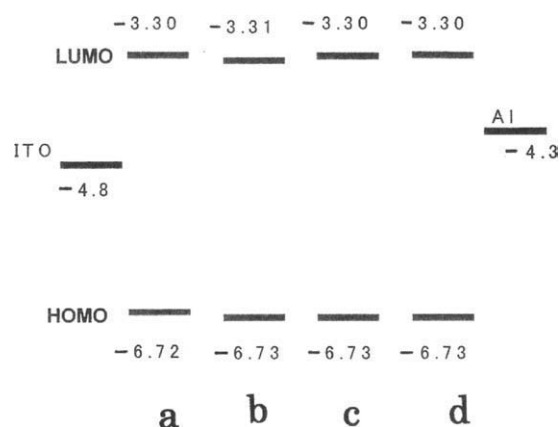


**Figure 7** Energy band diagrams of polymers **7** as determined from optical and electrochemical data.

**TABLE IV**  
Barrier Heights between Electrodes (Al and ITO) and Polyester-Imides **7**

Polymer	$\Delta E_h$ (eV) <sup>a</sup>	$\Delta E_e$ (eV) <sup>b</sup>	$\Delta E_{\text{bh}}$ (eV) <sup>c</sup>
7a	1.78	1.03	-0.75
7b	1.79	1.06	-0.73
7c	1.90	0.94	-0.96
7d	1.92	0.92	-1.00

<sup>a</sup>  $\Delta E_h = E_{\text{ITO}} (-4.8 \text{ eV}) - \text{HOMO}$ .

<sup>b</sup>  $\Delta E_e = \text{LUMO} - E_{\text{Al}} (-4.3 \text{ eV})$ .

<sup>c</sup>  $\Delta E_{\text{bh}} = \Delta E_e - \Delta E_h$ .

polymers **7c** and **7d** were higher than those of polymer **7a** and **7b**. This suggests that the DDPOD unit lead the polymers **7** to increase in  $E_e$  rather than  $E_h$  and stabilized the HOMO level, but the energy barriers between LUMO level values and work function of Al cathode ( $-4.3$  eV) were sufficiently small compared with the barriers in the DPTD-<sup>27,32</sup> and DPOD-containing polymers.<sup>33</sup> From these data, it is suggested that the polyester-imides (**7**) comprising the DDPOD moiety behave as electron-transporting materials for organic EL devices.

## CONCLUSIONS

New polyester-imides **7** having both DPOD and PI units (DDPOD moiety) were successfully prepared by the melt polycondensation of a dihydroxy derivative of DDPOD with four diesters in the presence of zinc acetate as a catalyst. Among them, the polymers **7c** and **7d** from aliphatic diesters **6c** and **6d** formed highly ordered thermotropic LC smectic phases. The resulting polymers **7** showed emission spectra with a bluish violet emission based on the DDPOD unit in the solutions and in the films and had stable HOMO levels, but were more sensitive to oxidation than polymers containing the electron-accepting DPOD unit. It was suggested that the polyester-imides **7** made up of DDPOD moiety in the backbones in this work not only have visible light-emitting properties together with LC properties, but also behave as electron-transporting materials for organic EL devices.

The authors thank Ms. Michiko Egawa for her help in obtaining the elemental analysis data.

## References

- Sato, M. In *Handbook of Thermoplastics*, Olabisi, O., Ed., Marcel Dekker: New York, 1997; p 665.
- Greiner, A.; Schmidt, H.-W. *Handbook of Liquid Crystals*, Demus, D., Goodby, J., Gray, G. W., Speiss, H.-W., Vill, V., Ed., John Wiley & Sons, Inc.: New York, 1998; Vol. 3, p 3.
- Inoue, T.; Kakimoto, M.; Imai, Y.; Watanabe, J *Macromol* 1995, 28, 6368.



4. Mikroyannidis, J. A. *Macromol Chem Phys* 1999, 200, 2327.
5. Spiliopoulos, I. K.; Mikroyannidis, J. A. *Macromolecules* 1998, 31, 515.
6. Pyo, S. M.; Kim, S. I.; Shin, T. J.; Park, H. K.; Ree, M.; Park, K. H.; Kang, J. S. *Macromolecules* 1998, 31, 4777.
7. Sato, M.; Nakamoto, Y.; Yonetake, K.; Kido, J. *Polym J* 2002, 34, 601.
8. Kricheldorf, H. R.; Gieseler, D.; Rabenstein, M. J. *Macromol Sci Pure Appl Chem* 2000, A37, 893.
9. Kukhta, A.; Kolesnik, E.; Taoubi, M.; Drozdova, D.; Prokopchuk, N. *Synth Met* 2001, 119, 129.
10. Du, F. S.; Cai, H.; Li, Z. C.; Li, F. M. *J Polym Sci A: Polym Chem* 1998, 36, 1111.
11. Ree, M.; Kim, S. I.; Pyo, S. M.; Shin, T. J.; Park, H. K.; Jung, J. C. *Macromol Symp* 1999, 142, 73.
12. He, X.; Liu, H.; Wang, N.; Ai, X.; Wang, S.; Li, Y.; Huang, C.; Cui, S.; Li, Y.; Zhu, D. *Macromol Rapid Commun* 2005, 26, 721.
13. Zhang, X.; Jin, Y. H.; Diao, H. X.; Du, F. S.; Li, Z. C.; Li, F. M. *Macromolecules* 2003, 36, 3115.
14. Sato, M.; Yoshinaga, T.; Koide, N. *Polym J* 2000, 32, 753.
15. Onimura, K.; Matsushita, M.; Yamabuki, K.; Oishi, T. *Polym J* 2010, 42, 290.
16. Akcelrud, L. *Prog Polym Sci* 2003, 28, 875.
17. Kim, S. W.; Shim, S. C.; Jung, B. J.; Shim, H. K. *Polymer* 2002, 43, 4297.
18. Ishii, J.; Sunaga, T.; Deguchi, S.; Tsukioka, M. *High Perform Polym* 2009, 22, 393.
19. Damaceanu, M. D.; Rusu, R. D.; Bruma, M.; Jarzabek, B. *Polym J* 2010, 42, 663.
20. Sato, M.; Ujiie, S. *Adv Mater* 1996, 8, 567.
21. El-Azhary, A. A. *Spectrochim Acta A* 1996, 52, 33.
22. Mochizuki, H.; Hasui, T.; Kawamoto, M.; Shiono, T.; Ikeda, T.; Adachi, C.; Taniguchi, Y.; Shirota, Y. *Chem Commun* 2000, 19, 1923.
23. Lami, H.; Laustriat, G. J. *Chem Phys* 1968, 48, 1832.
24. Schulz, B.; Bruma, M.; Brehmer, L. *Adv Mater* 1997, 9, 601.
25. Liu, Y. L.; Wang, K. L.; Huang, G. S.; Zhu, C. X.; Tok, E. S.; Neoh, K. G.; Kang, E. T. *Chem Mater* 2009, 21, 3391.
26. Sato, M.; Nakashima, A.; Sato, Y.; Yamaguchi, I. *J Polym Sci A: Polym Chem* 2008, 46, 6688.
27. Nakashima, S.; Sato, M.; Yamaguchi, I. *Polym Int* 2008, 57, 39.
28. Conwell, E. *Trends Polym Sci* 1997, 7, 218.
29. Mazur, S.; Lugg, P. S.; Yarnitzky, C. *J Electrochem Soc* 1987, 134, 346.
30. Viehbeck, A.; Goldberg, M. J.; Kovac, C. A. *J Electrochem Soc* 1990, 137, 1460.
31. Liu, Y.; Liu, M. S.; Jen, A. K.-Y. *Acta Polym* 1999, 50, 105.
32. Sato, M.; Tada, Y.; Nakashima, S.; Ishikura, K.; Handa, M.; Kasuga, K. *J Polym Sci A: Polym Chem* 2005, 43, 1511.
33. Yu, Y. H.; Chen, Y. *J Polym Sci A: Polym Chem* 2003, 41, 2765.
34. Li, H.; Zheng, Y.; Hu, Y.; Ma, D.; Wang, L.; Jin, X.; Wang, F. *Macromol Chem Phys* 2004, 205, 247.
35. Kim, J. H.; Lee, H. *Chem Mater* 2002, 14, 2270.
36. Thelakket, M.; Schmidt, H. W. *Adv Mater* 1998, 10, 219.